Mon. Not. R. astr. Soc. (1992) **258**, 705–714

Infrared imaging of *IRAS* sources near the Galactic Centre

Andrea Moneti,[1] Ian Glass[2] and Alan Moorwood[3]
[1]*European Southern Observatory, Casilla 19001, Santiago 19, Chile*
[2]*South African Astronomical Observatory, PO Box 9, Observatory, South Africa*
[3]*European Southern Observatory, Karl-Schwarzschild-Str. 2, D-8046 Garching, Germany*

Accepted 1992 April 14. Received 1992 April 9; in original form 1991 December 11

SUMMARY

A number of *IRAS* sources in the direction of the Galactic Centre and suspected of being regions of recent or current star formation have been investigated by means of direct near-infrared imaging and limited spectroscopy in a further attempt to clarify their nature. Near-infrared counterparts to the *IRAS* sources are selected from the various objects in the images on the basis of their near-infrared colours, coincidence with the 3.5-μm sources of Glass, and general appearance. Photometry is derived from the images, and combined with the spectroscopy and with previously published results to determine whether indeed these sources are close to the Galactic Centre and whether they are young. In general, the sources have cool energy distributions and luminosities of early-type ZAMS stars. Most of them share the properties of young massive stars still embedded in dust cocoons, though two of them appear to be surrounded by a compact H II region. The new results generally confirm our earlier conclusion that star formation is ongoing in the vicinity of the Galactic Centre.

Key words: stars: formation – Galaxy: centre – infrared: stars.

1 INTRODUCTION

Several lines of evidence suggest that star formation has occurred in the Galactic Centre over the last 10^8 yr, e.g., (i) the presence of supergiants in the Centre (Haller & Rieke 1989); (ii) the presence of compact radio continuum sources (CCS) near the Centre (Downes *et al.* 1978) which are probably compact H II regions; (iii) the fact that the ratio of the total ionizing flux to the total infrared luminosity is consistent with a normal rate of star formation (Cox & Laureijs 1989), and (iv) the increase in the number of luminous sources towards the Galactic Centre as implied by the colour–magnitude diagrams of Catchpole, Whitelock & Glass (1990) and the near-infrared brightness distribution of Rieke (1988). On the other hand, it is not clear how widespread star formation is at present times within about 50 pc of the Galactic Centre.

In order to address this question, Glass (1988, henceforth G88) searched the *IRAS* Point Source Catalog for sources within about 15 arcmin (or about 40 pc assuming a distance of 8.2 kpc) of the Centre and having *IRAS* colours typical of H II regions. He then used a single-channel photometer to perform an L-band ($\lambda = 3.5$ μm) search for their near-infrared counterparts and identified eight 'very red' (VR) objects ($K-L>2.0$) which he suggested could be the exciting and dust-heating stars of the H II regions. G88 worked mostly with 9- and 12-arcsec diameter apertures, and was thus subject to crowding problems. To confirm and improve G88's identifications, we have obtained seeing-limited near-infrared images of the *IRAS* fields using pixel scales of 0.8 and 0.5 arcsec. The sources of interest were identified on the basis of their $H-K$ colours: assuming a visual extinction of $A_V = 30$ mag to the Galactic Centre, and using the Rieke & Lebofsky (1985) reddening law, extinction alone would produce a colour excess $E(H\text{–}K) = 1.9$ mag. Our plan was thus to search for sources with $H\text{–}K \gtrsim 2$ in coincidence with the VR sources of G88, to obtain accurate positions and photometry, to obtain IR spectroscopy, and finally to combine the new data with those of G88 to elucidate further the nature of these objects.

We will present near-infrared images and selected spectroscopy of seven of G88's eight sources, and we will refer to them as VR 1–7. The correspondence between the VR number and the *IRAS* name can be found in Table 1. One of these objects, VR 5, consisting of a group of six or more bright sources and many other fainter ones, has already been studied in some detail (Glass, Moneti & Moorwood 1990, henceforth GMM; Nagata *et al.* 1990; Okuda *et al.* 1990).

2 OBSERVATIONS AND RESULTS

2.1 Infrared imaging

Direct infrared images were obtained at ESO/La Silla during 1989 June 16–21 and during 1990 July 28–August 3. The common-user Infrared Array Camera (IRAC) was used on the ESO/MPI 2.2-m telescope. Two slightly different engineering quality 32×32 Hg:Cd:Te arrays from Philips Components Ltd were used; the array available in 1990 was slightly better cosmetically, more stable with time, and generally yielded better results than the array used in 1989.

It should be noted that the Philips arrays are not optimized for astronomical observations: the sensitive part of each pixel is a small circular area comprising only ~ 15 per cent of the total pixel area, and located in the geometrical centre of the pixel. This results in a low total efficiency (~ 5 per cent at H for the atmosphere, telescope and camera combination), and in uncertainties in the photometry when the large pixel scales are used (see below), as large differences in the signal will occur when a star falls centred on a pixel and when it falls equidistant from four pixels. Furthermore, the short cut-off wavelength of the detector material, 2.3 μm, leaves the detector insensitive at the long-wavelength end of the K band.

Within IRAC are a filter and a lens wheel, both of which are cooled and remotely controlled. The filter wheel carries a set of ESO J, H and K filters, and a closed position used for bias and dark-current frames; the lens wheel carries four different objectives which yield pixel scales of 1.6, 0.82, 0.5 and 0.3 arcsec.

Bias frames were obtained throughout the observing run, and flat-fields were obtained on the evening and the morning sky for all necessary filter/lens combinations. The dark current of these arrays is negligible and was not accounted for.

Most of the science data were acquired in 'manual beam switch' mode: a frame obtained on a source was followed by another obtained with the same integration time on a reference sky position. A region of very low star density was identified on the K map of Glass, Catchpole & Whitelock (1987) at RA $17^h44^m31^s$, Dec. $-28°54'$ (2000), and was used for the reference exposures. Total integration times were of order 1–10 min. All observations were carried out under photometric conditions and the seeing varied between 1 and 2 arcsec.

In 1989 we conducted an initial *JHK* survey using the 1.6 arcsec per pixel scale in order to obtain a large field, and some further observations at higher spatial resolution were also obtained (see GMM). In 1990 we mostly followed up on the earlier observations by reobserving the regions at higher spatial resolution in order to improve on the photometry. All the images presented here were obtained in 1990. The large-field 1989 observations were used mostly in conjunction with the optical images (see below) for the determination of accurate positions for the infrared sources.

All images of stellar fields were reduced by subtracting the corresponding sky image, and by dividing the result by a normalized flat-field. In most cases the sky frame was first multiplied by a constant close to unity to compensate for slight variations in the sky brightness.

A montage of the images obtained at 0.82 arcsec pixel^{-1} resolution is shown in Fig. 1, while the 0.5 arcsec pixel^{-1} data are shown separately in Figs 2 (VR 5) and 3 (VR 6). In Fig. 1 the J-band images are shown across the top row and the H- and K-band images are in the centre and bottom rows, respectively. All images are shown with north to the top and east to the left, and each strip is 26 arcsec in the north–south direction. The images of VR 4 and 6 are mosaics of two adjacent and overlapping fields. The individual panels were normalized for display purposes; in particular, the intensity in the J and to a lesser degree the H images had to be amplified more than in the K images and as a result the noise in the sky is more prominent. Some obvious bad pixels were artificially removed in order not to distract the eye, but other defects were left in place, e.g. the dark band on the right side of VR 4-J. Fig. 2 shows, from left to right, J, H and K mosaics of VR 5. Here, the original frames were 16 arcsec on the side. These images were obtained under somewhat worse seeing conditions than the K-band image of this region shown in GMM (see the erratum for a good reproduction), though the new ones extend further south. The most important sources are identified in the K-band images; the numbering of the VR 5 sources follows that of GMM.

2.2 Photometry

Photometry was obtained from the reduced images by integrating the signal within a synthetic aperture whose size depended on the pixel scale used and on the local crowding. Standard stars from Elias *et al.* (1982) were observed throughout the night and normally on several different array positions. These were used to determine instrumental zero-points which were later used to calibrate the object photometry. The statistical uncertainty in the zero-point is 0.1 mag. Further systematic errors are due to the poorly known response curve of the detector, and to the use of standard star magnitudes based on a different photometric system. We expect that the combination of these should not exceed 0.1 mag in J and H. At K, the short cut-off wavelength of the detector material introduces a significant colour term in the photometry. We estimate that the K magnitudes for the reddest objects, such as sources 1 and 3 of GMM, will be ≈ 0.12 mag too high.

As the observations were mostly made at low airmass and in no cases at more than 2 airmasses, no atmospheric extinction corrections have been applied. Errors arising from this source should be considerably smaller than those already discussed. The new photometry of the more interesting sources is presented in Table 1. The photometry of G88 is also included for comparison.

2.3 Visible imaging

Direct images through a Gunn i filter were also obtained for all the fields and were used to determine accurate positions of the IR sources. The fields VR 1–5 were observed with a direct CCD camera on the Danish 1.5-m telescope, and the remaining fields were observed with the 3.5-m New Technology Telescope (NTT). Standard CCD reduction procedures consisting of bias subtraction and flat-fielding were applied to these images.

Accurate source positions were determined by comparing the IR images to the Gunn i images. In all cases, one or more visible stars could be identified in the J images, and in a few

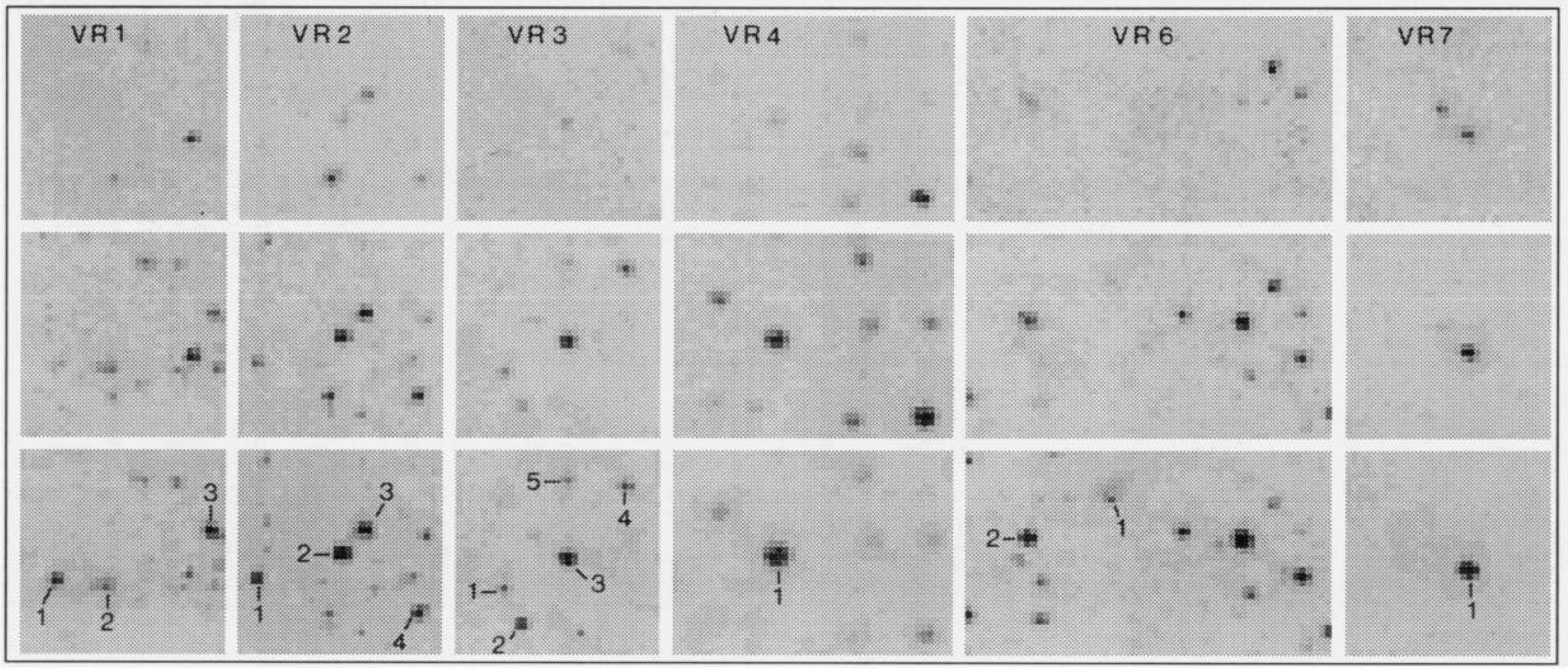

Figure 1. A montage of *J, H* and *K* images of the VR sources excluding VR 5. The *J*-, *H*- and *K*-band images are across the top, middle, and bottom rows, respectively. All images were obtained with a scale of 0.8 arcsec pixel^{-1}, and the vertical extent of each image is 32 pixels. In all cases north is to the top and east to the left. The sources of interest are identified.

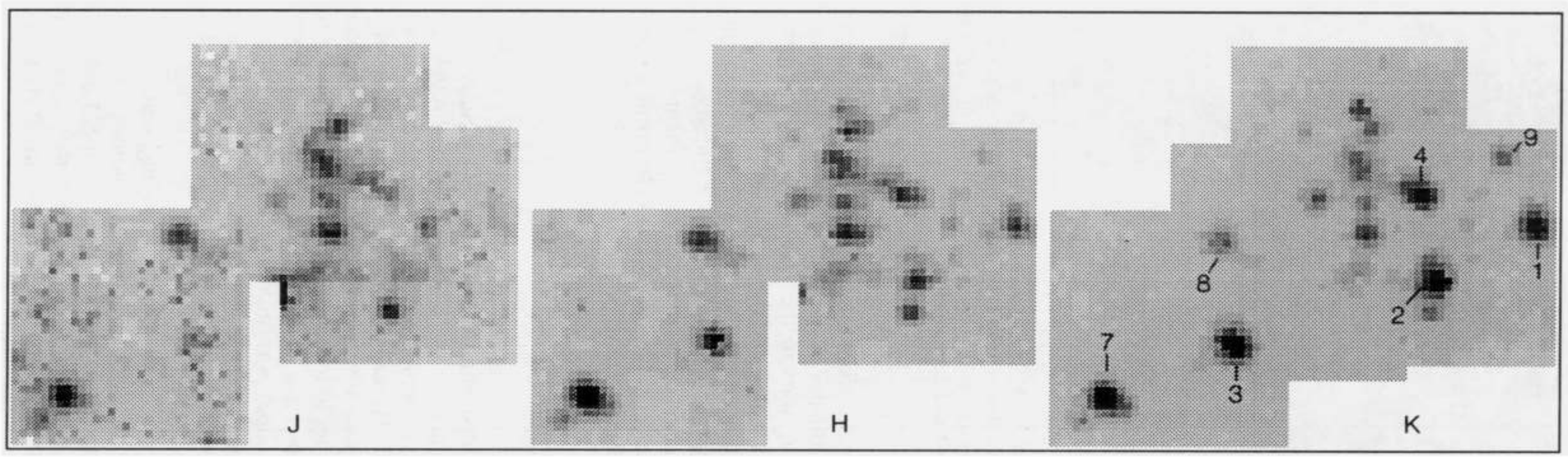

Figure 2. Similar to Fig. 1, but for VR 5. In this case, each panel is a mosaic of several images, and the data were obtained with a scale of 0.5 arcsec pixel^{-1}.

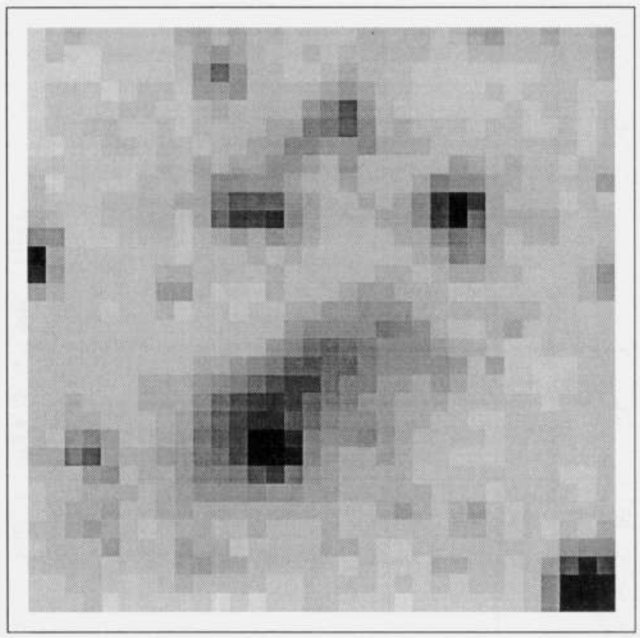

Figure 3. A *LK*-band image of the VR 6 region showing the ridge of extended emission. The scale is 0.5 arcsec pixel^{-1}, and the field is 16 arcsec on the side. North is to the top and east is to the left. VR 6-1 and 2 are labelled.

cases the visible star is also detected at longer wavelengths. Coordinates of the reference stars were obtained relative to nearby stars in the *Hubble Space Telescope* (*HST*) Guide Star Catalog, and the coordinates of the IR sources were then determined from the offsets in the infrared images. The final results should be accurate to ± 1 arcsec.

The positions of the most important sources are presented in Table 1. The *IRAS* and G88 positions are also included for completeness.

2.4 Infrared spectroscopy

Brγ observations of some of the brighter sources were obtained with IRSPEC, the ESO grating/array spectrometer, mounted on the 3.6-m telescope, through a 6-arcsec aperture. Chopping was used to remove the sky signal automatically. Typically, a chopping amplitude of 20 arcsec in declination was employed, but larger amplitudes were used at times to avoid objects known to be in the reference beam on the basis of the images. Beam switching (by moving the telescope) was used only for some of the observations. Rather, the chopping offset was carefully cancelled through observations of blank sky at the position of a strong atmospheric OH line.

To achieve proper sampling, each spectral line was observed with two grating positions corresponding to a half-pixel shift of the spectrum on the 32-element array. This could be done reliably given the accurate motion of the IRSPEC grating. The separate observations were then easily recombined in software.

The standard stars BS 7234 and 7515 were used for flux calibration. These stars have spectral type K1 III, and thus should have no Brγ line, either in emission or absorption, in their spectra (Kleinmann & Hall 1986). The instrumental sensitivity was determined by fitting the 1–5 μm energy distribution of the standards, as determined by their broad-band magnitudes, and dividing that by the raw counts at each wavelength of observation. The result was then fitted by a third-degree polynomial in order to remove the weak features present in the raw spectra of the standard stars, and was finally multiplied by the source counts to obtain a flux-calibrated spectrum.

The Brγ spectra are shown in Fig. 4. Strong Brγ emission was detected in VR 7, while no significant emission was detected in VR 2, 3, and 4. Spectroscopy of the brighter VR 5 sources and of VR 6-1 was also attempted, but no reliable measurements were obtained due to contamination from emission in the reference beam. For VR 7, a line intensity of 2.1×10^{-16} W m^{-2} was determined by fitting a

Table 1. Source data.

Source id	R.A. (2000)	Dec. (2000)	K	H–K	J–H
VR 1 (IRAS 17417 –2851)					
IRAS	17 44 53.3	–28 52 20			
G88	17 44 54.7	–28 52 07	11.2	3.3	
1	17 44 54.6	–28 52 04	11.3	4.2	
2	54.1	52 05	11.7	1.5	1.9
3	53.4	51 44	10.9	2.6	
VR 2 (IRAS 17423 –2855)					
IRAS	17 45 29.4	–28 56 11			
G88	17 45 28.8	–28 56 04	8.8	2.2	3.6
1	17 45 29.7	–28 56 11	10.1	2.7	
2	28.9	08	9.1	2.4	4.2
3	28.7	05	9.5	2.1	
4	28.1	16	9.9	2.0	
VR 3 (IRAS 17428 –2854)					
IRAS	17 46 00.6	–28 55 26			
G88	17 45 59.6	–28 55 26	10.2	3.8	
1	17 45 59.6	–28 55 18	10.3	2.6	
2	59.4	22	9.6	3.4	
3	59.0	14	9.0	2.4	5.1:
4	58.4	05	10.3	2.1	3.9
5	59.0	04	10.9	3.0	
VR 4 (IRAS 17430 –2851)					
IRAS	17 46 11.4	–28 52 58			
G88	17 46 04.5	–28 52 52	7.4	2.8	
1	17 46 04.4	–28 52 50	7.4	3.2	4.6
VR 5 (IRAS 17430 –2848)					
IRAS	17 46 13.8	–28 49 48			
G88-A	17 46 14.1	–28 49 38	7.6	3.3	
G88-B	17 46 14.7	–28 49 43	6.0	3.0	3.9
G88-C	17 46 15.9	–28 49 48	7.0	3.3	
1	17 46 14.2	–28 49 39	7.8	3.4	
2	14.8	43	7.3	3.5	5.4
3	15.8	47	7.1	3.5	5.1
4	14.8	37	7.7	3.1	
5	15.1	31	9.1	3.3	
7	16.4	51	7.3	2.3	4.5
8	15.9	40	9.2	1.8	4.0
9	14.4	34	9.4	3.8	
VR 6 (IRAS 17433 –2838)					
IRAS	17 46 28.5	–28 39 23			
G88	17 46 29.2	–28 39 22	9.8	3.0	
1	17 46 28.2	–28 39 23	10.9	2.8	
2	29.0	39 28	9.9	2.4	
VR 7 (IRAS 17434 –2858)					
IRAS	17 46 35.8	–28 59 58			
G88	17 46 34.7	–28 59 59	7.4	2.4	
1	17 46 34.5	–28 59 57	7.5	2.4	4.1

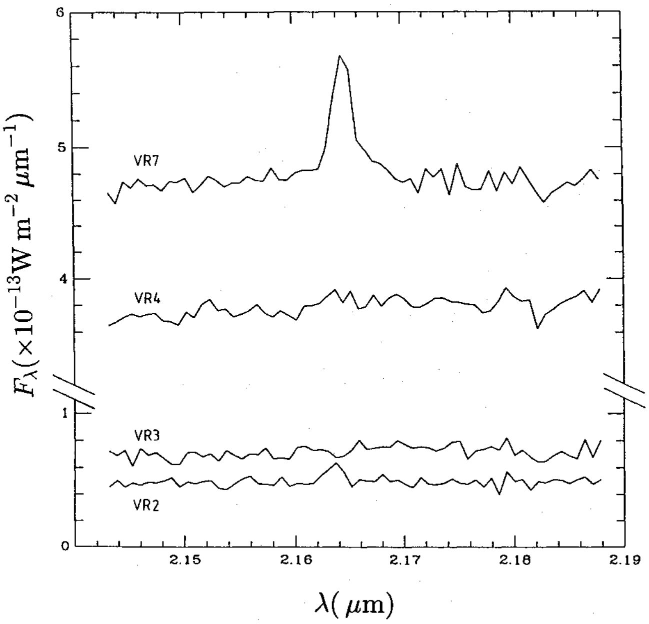

Figure 4. Flux-calibrated Brγ spectra of selected VR sources.

Gaussian profile over a sloping continuum. The formal uncertainty for the Brγ measurements, as determined from the fit, is $\sigma \sim 0.2 \times 10^{-16}$ W m^{-2}. In all cases, the measured continuum is comparable to that determined from the photometry.

3 DISCUSSION

We begin by considering which of the near-IR sources found in each field is the most likely counterpart of the *IRAS* source. This will be done on the basis of its colour, spatial coincident with an L source from G88, and the presence of extended emission. Note that the density of stars in the K images is sufficiently high that the 9- and 12-arcsec diameter apertures of G88 included more than one object in almost all cases. At L, however, cool sources (i.e. $\lesssim 1000$ K) whose energy distributions peak in this band, will be more prominent than normal stars. It follows that the L photometry of G88 should not in general be contaminated by spurious sources along the line of sight.

3.1 The individual fields

3.1.1 VR 1 (IRAS 17417 – 2851)

The reddest IR source in this field is VR 1-1. About 8 arcsec west of VR 1-1 is a second source, VR 1-2, which is clearly extended in both the H and the K images and which is also detected at J. VR 1-2 is much brighter than VR 1-1 in H and in J, and it has rather peculiar near-IR colours which are not consistent with a reddened photosphere. The position of the G88 counterpart coincides with our VR 1-1, as does the K magnitude. G88, however, gives $H-K=3.3$ mag compared to our 4.2 mag. This can be explained if his 9-arcsec beam accepted some emission from VR 1-2. VR 1-1 lies 16 arcsec north of the *IRAS* position, or well outside the error box. Our low-resolution 1989 data do not reveal any other possible counterparts within the error box.

On the basis of its $(H-K)$ colour and its positional coincidence with the L-band source of G88, we conclude the most likely counterpart of the *IRAS* source is VR 1-1, even though it lies outside the *IRAS* error box. Due to its extended emission, however, VR 1-2 should not be discarded.

This region was searched for H_2O maser emission (Braz *et al.* 1989), but none was found.

3.1.2 VR 2 (IRAS 17423 – 2855)

The VR 2 field is rather crowded: there are four sources with $K \lesssim 10$ mag and $H-K \gtrsim 2.0$ mag. Of these, VR 2-1 is the reddest, while the L-band source of G88 coincides with the combination of VR 2-2 and 2-3. Our combined H and K photometry of these two sources is in excellent agreement with that of G88. Furthermore, VR 2-3 appears slightly extended in the K image. All three sources lie within the *IRAS* error box which is centred 9 arcsec east and 6 arcsec south of VR 2-3, and which coincides with the location of CCS no. 14 of Downes *et al.* (1979). There is no conspicuous near-IR source at that position. On the basis of the G88 position and its extended appearance, we suggest that VR 2-3 is the counterpart to the *IRAS* source. The *IRAS* source, however, could be a blend of some or all of VR 2-1, 2, and 3.

It is worth noting that an LRS spectrum of the *IRAS* source (Volk & Cohen 1989) shows a steep red continuum with a deep silicate absorption feature at 9.7 μm.

3.1.3 VR 3 (IRAS 17428 – 2854)

Here also there are several sources in the field. VR 3-2 is the second brightest at K and the reddest in $(H-K)$, and it falls within G88's aperture. VR 3-1 is fainter and also falls within G88's aperture. Curiously, the source in G88 is 0.5 mag fainter at K than VR 3-2 and it is redder in $(H-K)$; this behaviour cannot be explained by combining the photometry of VR 3-2 and of VR 3-1. The location of VR 3 is on the border of the area surveyed by Downes *et al.* (1979), and it is not clear whether it was included.

3.1.4 VR 4 (IRAS 17430 – 2851)

Our best candidate for the counterpart of this source is an isolated bright ($K=7.4$) and red ($H-K=3.2$) source at the western end of the *IRAS* error box, VR 4-1. The position given in G88 is that of a less red star nearer to the *IRAS* position; however, the published photometry is of the correct object whose coordinates were measured at the time and are reported correctly in Table 1. Our photometry is in excellent agreement with that of G88 and leaves little doubt that this is the same source. The CCS no. 18 of Downes *et al.* (1979) is located 18 arcsec west of VR 4-1. That distance is such that a physical association between the two is unlikely.

3.1.5 VR 5 (IRAS 17430 – 2848)

This field corresponds to the cluster that has already been discussed in GMM and in Nagata *et al.* (1990) and Okuda *et al.* (1990); this source is also known as AFGL2004. Our data are shown in Fig. 2 and cover a larger area than the images of Nagata *et al.* (1990). They show that what these investigators called a 'quintuplet' actually contains six bright sources, the sixth being located further west than the object they called GCS-4 (our VR 5-3). We also provide J and H images of the region. A larger scale K image kindly obtained by Dr R. Catchpole (private communication) with a Nicmos-2 128×128 array and covering a field of 3.8×3.8 arcmin^2 does not reveal other bright objects in the immediate vicinity of the cluster. The characteristic dimension of the cluster is ~20 arcsec.

The *IRAS* position is about 10 arcsec south and 8 arcsec west of VR 1-1, and only VR 1-2 falls within the formal *IRAS* error box. The LRS spectrum of the *IRAS* source (Volk & Cohen 1989) shows a steeply rising continuum with a deep 9.7-μm silicate feature. G88's sources A, **B** and C in this field correspond to our sources VR 5-1, 2 and 3, respectively. The new photometry of these and of the remaining sources agrees to within 0.2 mag with the 6-arcsec diameter aperture photometry of GMM.

Nagata *et al.* (1990) remarked on the diffuse emission within the cluster. However, we believe that what they saw was composed of the blended images of several faint stars which can be seen in the data of GMM (see reproduction in the erratum). This conclusion is supported by a deeper, but lower resolution image obtained with the SAAO infrared camera, which does not reveal any extended emission on a larger scale.

Okuda *et al.* (1990) failed to detect any emission or absorption features in the near-infrared spectra of VR 5-2 and 5-3. However, they did observe deep 9.7-μm silicate absorption in VR 5-1, 2, 3, 4, and 9 using narrow-band filters, and they adopt an extinction of $A_V = 20$–25 mag. Okuda *et al.* also noted the proximity (in projection) of the cluster sources to the bright 5-GHz radio feature known as the 'pistol' (Yusef-Zadeh & Morris 1987), which is located about 20 arcsec south of the main body of the cluster. The strongest peaks of the pistol correspond to CCSs nos. 27 and 29 of Downes *et al.* (1979). No K-band emission from the pistol is present in the image of R. Catchpole. On the other hand, Yusef-Zadeh, Telesco & Decher (1989) did detect 10-μm emission from the strongest peaks of the pistol, though at a much lower level than the emission from the cluster sources themselves. This connection suggests a relation between the pistol and the cluster, though more extended studies of the 10-μm emission in the region are necessary to confirm this.

3.1.6 *VR 6 (IRAS 17433 – 2838)*

This field, shown in detail in Fig. 3, shows a moderately bright ($K = 10.9$) and moderately red ($H - K = 2.8$) source, VR 6-1, located on the edge of a ridge of diffuse emission running NW–SE and about 15 arcsec long. During our spectroscopic run we noted some Brγ emission from the vicinity of this source, but the region was very confused and could not be studied in detail. Still, the extended emission may be an H II region, making this source the most likely counterpart to the *IRAS* source.

A recent deep K image of this field obtained with the SAAO infrared camera reveals that VR 6-1 and the nebulosity near it are themselves superimposed on an area of fainter nebulosity extending over a region of 20×18 arcsec^2. The centre of the faint nebulosity is about 5 arcsec north-north-east of VR 6-1. It overlaps partly with CCS no. 45, which has a diameter of 26 arcsec but is not completely coincident with it. It is unclear whether the IR nebulosity and the extended CCS are related. If they are, the incompleteness of the overlap could be due to a band of high extinction close to the source itself.

The G88 source is not coincident with VR 6-1 but rather with VR 6-2 which is also very red. Both sources fall within the *IRAS* error box, so that the *IRAS* source is likely to be a composite one.

3.1.7 *VR 7 (IRAS 17434 – 2858)*

An isolated bright source is the probable counterpart of the *IRAS* source. Our position is in good agreement with both the *IRAS* position and with that of G88. Our photometry is also in good agreement with that of G88. The region of this source was not surveyed by Downes *et al.* (1979).

3.2 Relationships to molecular clouds and other radio features

The density of molecular material in the line of sight to these sources is extremely high and it is not possible to identify individual clouds with the VR sources due to the comparatively low spatial resolution, 2 arcmin, of the best existing molecular line maps (Bally *et al.* 1988). In the case of the brighter VR 5 sources, however, Okuda *et al.* (1990) present velocity-resolved spectroscopy showing absorption components from several clouds at negative radial velocities which may form part of the 200-pc expanding molecular ring (Sofue 1989). The apparent visual extinction of $A_V \approx 30$ mag implies that the ^{13}CO in the line of sight cannot be more than 15 K km s^{-1} (Glass *et al.* 1987), and thus that the sources VR 2, 3, 4, 5 and 6 lie in front of all, or almost all, of the positive-velocity material.

All the VR sources are located over the diffuse radio emission that is present in the Galactic Centre as seen, for instance, in the large-scale radio continuum maps of Altenhoff *et al.* (1979). The coincidences with the CCSs of Downes *et al.* (1979) have already been discussed, and possible coincidences with other features in more recent radio continuum maps will be discussed in a future work.

3.3 The field stars

During the course of the survey many field stars were detected which are along the line of sight to the sources of interest. Here we analyse how these and the *IRAS* counterparts behave in the $(J-H)$ versus $(H-K)$ diagram which is shown in Fig. 5. There, the field stars are represented by empty squares, and the *IRAS* counterparts by filled ones. The reddening line is shown extending from the locus of late-type giant stars. The locus of (unreddened) blackbodies with different temperatures is also shown for comparison. Unfortunately, the latter is nearly parallel to the reddening line, making it impossible to disentangle the effects of reddening from those of intrinsic temperature.

In general all the sources follow the reddening line, albeit with some dispersion. Nearly all the VR sources are found in the reddest part of the diagram, as they were selected on the basis of $H - K \gtrsim 2$ mag. The main exception, VR 1-2, was

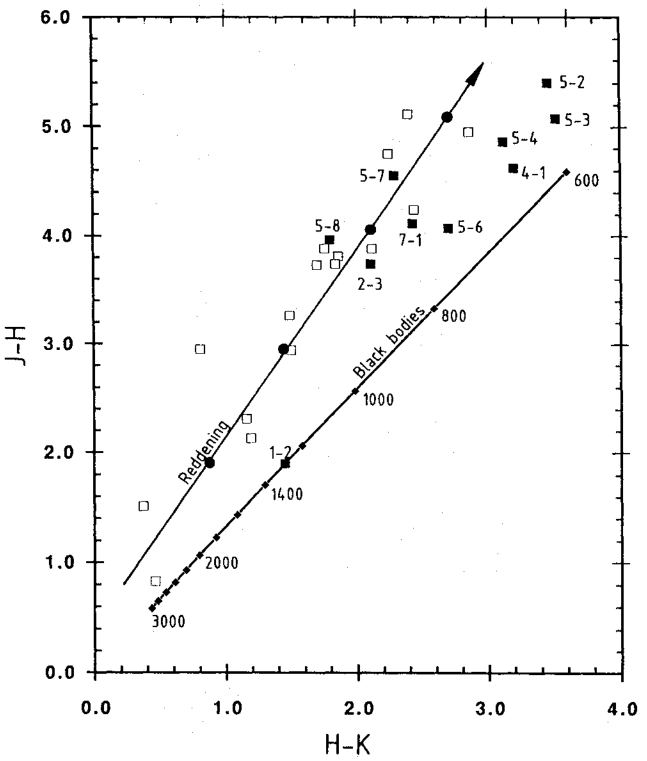

Figure 5. $(J-H)$ versus $(H-K)$ colour–colour diagram for all sources with J, H and K photometry. Filled symbols indicate VR sources, empty symbols are the field stars. Most VR sources are labelled, the unlabelled ones are two faint members of the VR 5 cluster. A reddening line extending from the locus of late-type stars is shown and it is marked at intervals corresponding to $A_V = 10$ mag. The locus of (unreddened) blackbodies is also displayed; it is marked with the corresponding temperature in intervals of 200 K, and a few positions are labelled with the temperature.

selected on the basis of its extended nature, and indeed it turns out to have colours rather untypical of a reddened star. A total of 16 field stars are present in Fig. 5. Of these, 11 have $1.5 \lesssim H-K \lesssim 3.0$ mag which, assuming an intrinsic colour of $H-K \gtrsim 0.2$ mag, typical of nearly all stars and indeed of blackbodies with $T_{BB} \gtrsim 2500$ K, would imply an extinction of $25 \lesssim A_V \lesssim 50$ mag, using the Rieke & Lebofsky (1985) reddening law. The remaining five stars are likely to be foreground.

Overall, the *IRAS* counterparts are not clearly distinguishable from field stars in this plot, and the *IRAS* counterparts that are reddest in $(H-K)$, and which potentially might show a larger displacement from the reddening line, are simply too faint at J for detection and do not appear on this diagram. Only for $J-H \gtrsim 4$ mag do the VR sources fall consistently to the right of the reddening line.

3.4 The location of the VR sources

The evidence that the VR sources as a group are indeed in the Galactic Centre is derived from their spatial distribution. We have analysed 13 circular fields of 0°.25 radius centred on the Galactic latitude and longitude axes, and separated by 0°.50 each. The *IRAS* 12-, 25- and 60-μm fluxes, F_{12}, F_{25} and F_{60} respectively, have been used to separate sources into the categories of indeterminate, stellar, and nebulous objects, with the last category including the characteristics of H II regions and planetary nebulae. Assuming that there are no external galaxies in the fields, the two-colour diagram presented by Pottasch (1987) may be used as follows:

(i) if $F_{12}/F_{25} > 0.3$ the source is a star;
(ii) if $F_{12}/F_{25} < 0.3$ the source is a nebulous object, and
(iii) if there is no reliable F_{12}/F_{25} and $F_{25}/F_{60} < 0.2$, the source is possibly an H II region.

The average 12-μm flux from each field was also determined. The value of this is occasionally distorted by a few, presumably foreground, stellar sources. The result of this analysis is displayed in Fig. 6. It will be seen that away from the plane of the Galaxy there are few nebulous sources, and the classifications of these are uncertain. Most of the sources away from the lane are demonstrably stars. While the above result shows that the nebular sources lie close to the Galactic plane, the distribution of sources in the longitudinal direction is less clear-cut, but it is definitely peaked at the Centre. The ratio of the number of stellar sources to the number of nebulous sources varies from 7.5 to 0.4 as we go from the Centre to 1°.5 away. This striking difference may be enhanced somewhat if the 'uncertain' nebulous sources turn out to be stellar, or diminished if the indeterminate sources are H II regions, but will exceed 3:1 in the worst case.

The average 12-μm flux also shows a striking peak towards the central field, even though the Central Source, IRAS 17424 − 2859, has been omitted from the average of that field. Some of the averages have been affected by the presence of a few exceptionally bright sources (see particularly the field at $l^{II} = -1°.5$ and $b^{II} = 0°.0$) whose colours are typical of stars. The VR sources considered in this paper tend to be bright at 12 μm (10.7, 178, 11.5, 7.5, 213, 36 and 13.8 Jy for VR 1-7 respectively), and thus are probably part of the luminous population directly associated with the Centre. Furthermore, six of the seven sources under consideration are in the central field and the remaining one, VR 6, is in the $l^{II} = 0°.5$ and $b^{II} = 0°.0$ field. In fact, the six VR sources in the central field make up nearly one third of the total number of *IRAS* sources in that field.

We conclude that the evidence that the VR sources are indeed located in the Galactic Centre remains for the most part circumstantial, but on the whole it is fairly convincing. In the case of VR 5 sources, the CO absorption spectroscopy (see Section 3.2) and the infrared polarization of these sources (Okuda *et al.* 1990) provides further evidence for their location close to the Centre.

3.5 Spectral energy distribution

We have combined our J, H and K data with the L, M and N photometry of G88 and of Nagata *et al.* (1990) and with the *IRAS* data in order to plot the spectral energy distributions (SEDs) of the sources under study. These are shown in Fig. 7. The ground-based data were dereddened by $A_V = 30$ mag for most sources and by $A_V = 22$ mag for the VR 5 cluster (see GMM) using the Rieke & Lebofsky (1985) reddening law. The *IRAS* data were not dereddened, and upper limits were not plotted. The *IRAS* data were not plotted for the cluster sources, since we cannot separate the *IRAS* fluxes into the different cluster components; at any rate, only a

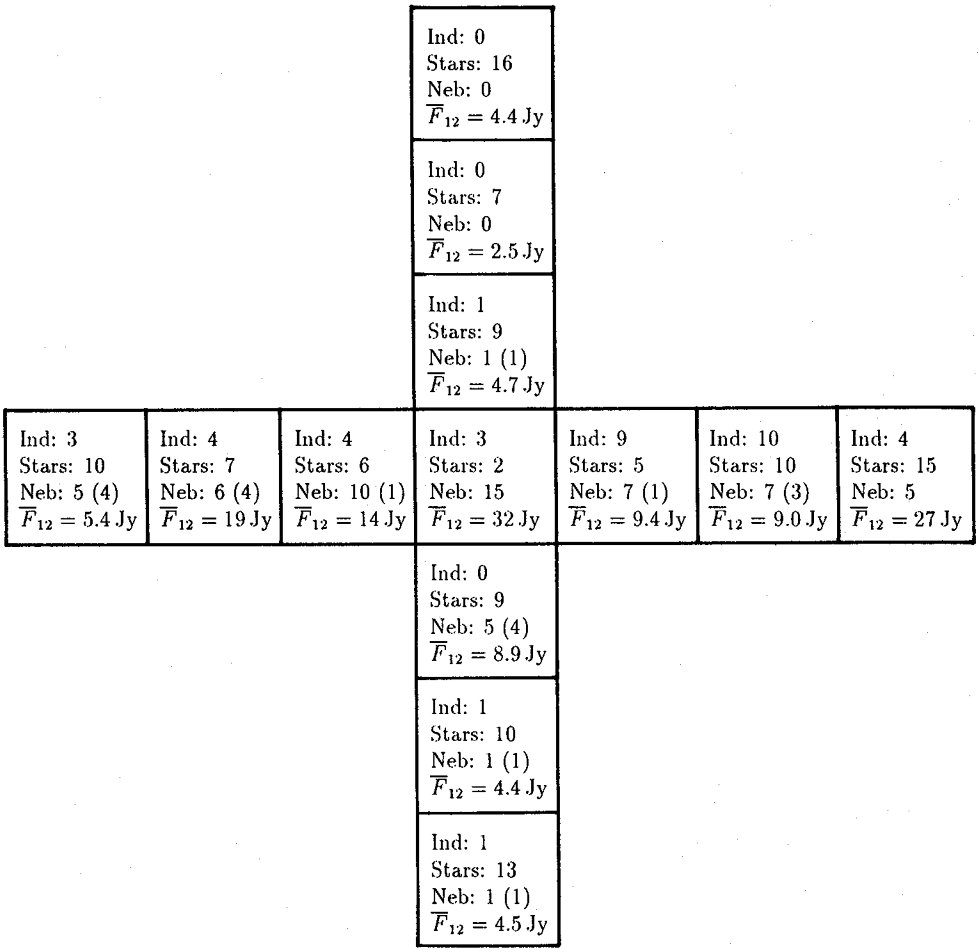

Figure 6. Contents of 0°25 diameter *IRAS* fields near the Galactic Centre. The fields are spaced by 0°25 in Galactic latitude and longitude, as described in the text. Galactic longitude increases to the left, and latitude upwards. Ind: = indeterminate type object, Neb: = H II region or planetary nebula. The numbers of uncertain nebulous classifications are given in parentheses. $\overline{F}_{12}$ is the average 12-μm flux of the sources in that field. Note that IRAS 17424 − 2859, corresponding to the Galactic Centre source itself, was omitted from the determination of $\overline{F}_{12}$ for the central field.

12-μm point is given for the cluster while the remaining points are upper limits.

The SEDs of VR 1, 4, 6, and 7 clearly increase toward long wavelengths and peak beyond 100 μm. Note that for VR 4, 6, and 7 only upper limits are given at 25 μm. The SEDs of VR 2 and 3 are only plotted out to 60 and 25 μm respectively, as only upper limits are given beyond those wavelengths. The SED of VR 2 appears to flatten out at 60 μm, while that of VR 3 is still increasing at 25 μm.

To determine apparent bolometric magnitudes, m_{bol}, and effective temperatures, T_{BB}, of the VR sources we have fitted the spectral energy distributions with Planck functions. Fig. 7 shows the blackbody fits, and the numerical results are given in Table 2. The choice of the blackbody curves to approximate the energy distributions is purely arbitrary and represents a method for extrapolation to wavelengths where we have no real knowledge of the true values of F_ν. The *IRAS* photometry was not used in the fits, since: (i) in many cases only upper limits are given, and (ii) they can be contaminated by spurious sources falling in the large *IRAS* beam. Including the *IRAS* photometry, where available, would make the sources 1–2 mag brighter in m_{bol}.

The amounts of reddening for the individual sources cannot be determined very precisely. However, because of their low temperatures, which imply that their energy distributions peak at long wavelengths (> 3 μm) where the extinction coefficients are small, a change in A_V has only a minor effect on m_{bol} and on T_{BB}. For example, VR 5-1 at $A_V = 30$ mag yields $m_{bol} = 7.7$ mag and $T_{BB} = 720$ K, whilst at $A_V = 22$ mag it has $m_{bol} = 7.4$ mag and $T_{BB} = 780$ K.

3.6 The nature of the VR sources

We begin by considering the cluster sources, for which the largest amount of data is available. Their bolometric magnitudes are appropriate for zero-age main-sequence (ZAMS) stars between spectral types B3 and O8, and the low T_{BB}s suggest that these objects are surrounded by optically thick dust cocoons which are absorbing the hot stellar radiation and reradiating in the infrared. Okuda *et al.* (1990) note that the polarization appears to be interstellar rather than intrinsic to the source, and the extinction derived from it is consistent with the depth of the silicate features. The homogeneity of the silicate feature depth and of the polarization

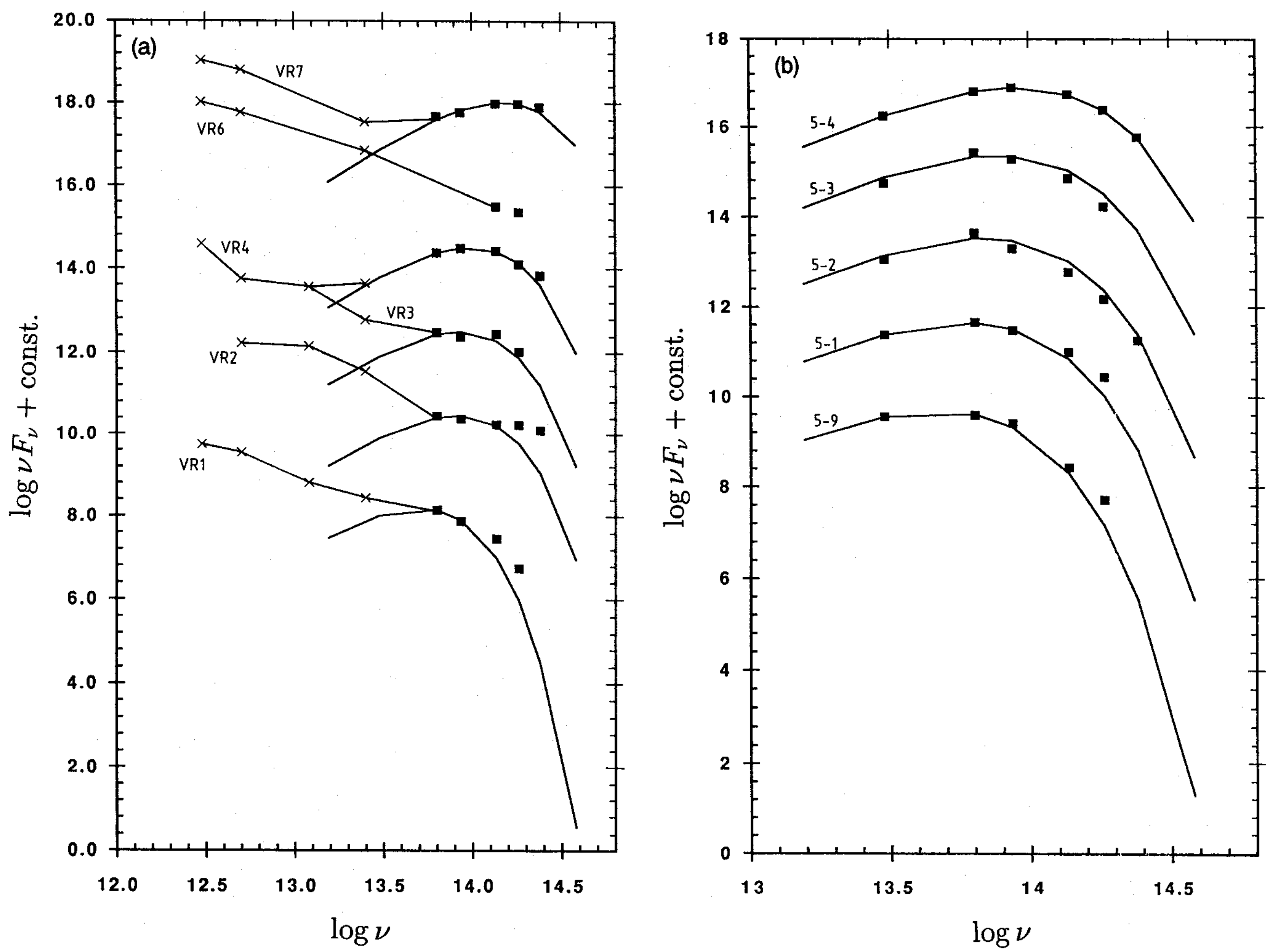

Figure 7. Spectral energy distributions and blackbody fits of the VR sources compiled using *J, H* and *K* photometry from this work, *L* and *M* photometry from G88, and *N* photometry from Nagata *et al.* (1990).

Table 2. Bolometric magnitudes and temperatures.

Source	m_{bol}	T_{BB}	M^*_{bol}
VR1-1	10.3	620	-4.2
VR2-2	9.4	1010	-5.2
VR3-2	10.3	1050	-4.3
VR4-1	8.0	1210	-6.6
VR5-1	7.7	720	-6.9
VR5-2	6.9	830	-7.6
VR5-3	7.4	940	-7.2
VR5-4	8.6	1110	-6.0
VR5-9	7.8	580	-6.7
VR6-1	10.3	1070	-4.3
VR7-1	9.1	1270	-5.5

*For a distance modulus of 14.57.

also suggests that these must arise from foreground material rather than from circumstellar effects. Since the extinction to the cluster sources is comparable to that of other sources toward the Centre, the cluster does not appear to be deeply embedded in a molecular cloud, which argues against extreme youth. On the other hand, the high luminosity and especially the clustering argue in favour of youth, as does the absence of photospheric CO absorption in two of the cluster members (Okuda *et al.* 1990), which indicates that they are not late-type, evolved objects. We suggest that these sources are indeed young, i.e. $\lesssim 10^6$ yr old, but that they are probably not typical young stellar objects.

The objects VR 2 and 7 are also of special interest, since they are associated with ionized gas: VR 2 is coincident with Downes *et al.* (1979)'s CCS no. 14, and VR 7 has strong Brγ emission. These two sources could be compact H II regions: the infrared luminosity of a compact H II region is related uniquely to the expected radio continuum and to the hydrogen recombination line fluxes using case B conditions and the emission rate of ionizing radiation from the exciting star(s) (see, for instance, Moorwood & Salinari 1983). For VR 7-1 we have a Brγ flux of 2×10^{-15} W m^{-2} after correcting for $A_V \approx 30$ mag. At the distance of 8.2 kpc this yields (for case B) $n_e^2 V \approx 5\times10^{59}$ cm^{-3}, where n_e is the electron density and V the volume of the region. This corresponds to a B0 star of $M_{bol} = -6$ mag, which is reasonably close to our value of $M_{bol} \approx -5.5$ mag. The VR 2/CCS 14 source has $F_{5\,GHz} = 0.2$ Jy (Downes *et al.* 1979), from which we derive an $n_e^2 V = 7\times10^{58}$ cm^{-3} which corresponds to an $M_{bol} = -5.3$ mag, close to our value of -5.2 mag. However, Brγ should have been detected with an intensity of 1.8×10^{-16} W m^{-2}

after dereddening for $A_V = 30$ mag, or about three times our upper limit. Apart from the possibility of observational errors, the line flux may be reduced by internal reddening or by the non-applicability of case B.

Data on the remaining objects are somewhat more scarce, but their luminosities and energy distributions are generally consistent with those of deeply embedded massive stars.

4 CONCLUSION

We have presented further observations of suspected young sources in the vicinity of the Galactic Centre. The total luminosities and the spectral energy distributions of the sources generally corroborate our earlier conclusions that these sources are very young: several may be objects that are still deeply embedded in the molecular clouds out of which they condensed, while others appear to be somewhat more evolved, either by showing a clear assocation with a (probably compact) H II region or by showing that they are not deeply embedded. We thus can conclude that stars are forming in the vicinity of the Galactic Centre.

REFERENCES

Altenhoff, W. J., Downes, D., Pauls, T. & Schraml, J., 1979. *Astr. Astrophys. Suppl.*, **35**, 23.

Bally, J., Stark, A. A., Wilson, R. W. & Henkel, C., 1988. *Astrophys. J.*, **324**, 223.

Braz, M. A., Scalise, E., Hetem, J. C. G., Monteiro do Vale, J. L. & Gaylard, M., 1989. *Astr. Astrophys. Suppl.*, **77**, 465.

Catchpole, R. M., Whitelock, P. A. & Glass, I. S., 1990. *Mon. Not. R. astr. Soc.*, **247**, 479.

Cox, P. & Laureijs, R., 1989. In: *The Center of the Galaxy, IAU Symp. No. 136*, p. 121, ed. Morris, M., Kluwer, Dordrecht.

Downes, D., Goss, W. M., Schwarz, W. & Wouterlout, J. G. A., 1978. *Astr. Astrophys. Suppl.*, **35**, 1.

Elias, J. H., Frogel, J. A., Matthews, K. & Neugebauer, G., 1982. *Astr. J.*, **87**, 1029.

Glass, I. S., 1988. *Mon. Not. R. astr. Soc.*, **234**, 115 (G88).

Glass, I. S., Catchpole, R. M. & Whitelock, P. A., 1987. *Mon. Not. R. astr. Soc.*, **227**, 373.

Glass, I. S., Moneti, A. & Moorwood, A. F. M., 1990. *Mon. Not. R. astr. Soc.*, **242**, 55P (also erratum, **244**, 767) (GMM).

Haller, J. W. & Rieke, M. J., 1989. In: *The Center of the Galaxy, IAU Symp. No. 136*, p. 487, ed. Morris, M., Kluwer, Dordrecht.

Kleinmann, S. G. & Hall, D. N. B., 1986. *Astrophys. J. Suppl.*, **62**, 501.

Moorwood, A. F. M. & Salinari, P., 1983. *Astr. Astrophys.*, **125**, 342.

Nagata, T., Woodward, C. E., Shure, M., Pipher, J. L. & Okuda, H., 1990. *Astrophys. J.*, **351**, 83.

Okuda, H., Shibai, H., Nakagawa, T., Matsuhara, H., Kobayashi, Y., Kaifu, N., Nagata, T., Gatley, I. & Geballe, T. R., 1990. *Astrophys. J.*, **351**, 89.

Pottasch, S. R., 1987. In: *Planetary and Proto-Planetary Nebulae: from IRAS to ISO*, p. 1, ed. Preite-Martinez, A., Reidel, Dordrecht.

Rieke, M. J., 1988. In: *Galactic and Extragalactic Star Formation*, p. 345, eds Pudritz, R. E. & Fich, M., Kluwer, Dordrecht.

Rieke, G. H. & Lebofsky, M. J., 1985. *Astrophys. J.*, **288**, 618.

Sofue, Y., 1989. In: *The Center of the Galaxy, IAU Symp. No. 136*, p. 213, ed. Morris, M., Kluwer, Dordrecht.

Volk, K. & Cohen, M., 1989. *Astr. J.*, **98**, 931.

Wynn-Williams, C. G., 1982. *Ann. Rev. Astr. Astrophys.*, **20**, 587.

Yusef-Zadeh, F. V. & Morris, M., 1987. *Astr. J.*, **94**, 1178.

Yusef-Zadeh, F. V., Telesco, C. M. & Decher, R., 1989. In: *The Center of the Galaxy, IAU Symp. No. 136*, p. 287, ed. Morris, M., Kluwer, Dordrecht.